

# Response characteristics of surface inclinometers during slope failure and influence of installation conditions

Yoko Ohta, Yukio Nakata

Graduate School of Sciences and Technology for Innovation, Yamaguchi University, Japan, [y\\_ohta@yamaguchi\\_u.ac.jp](mailto:y_ohta@yamaguchi_u.ac.jp)

**ABSTRACT:** Frequent heavy rains in recent years have increased the risk of landslides, and advanced monitoring techniques are needed to assess slope stability. Surface inclinometers are gaining attention as a promising tool for detecting slope movements. However, fundamental data on their response remains insufficient. This study aims to investigate the response characteristics of surface inclinometers during slope failure and the influence of installation conditions on their response. A series of slope failure experiments was conducted using a model slope with a height of 200 mm and an inclination of 25 degrees, made from dry Toyoura sand. Five inclinometers were installed along the model slope. To verify how the installation conditions influenced the inclinometer's response, the instrument length varied to 25 and 45 mm, while the depth from the slope surface varied to 10, 20, and 30 mm. After preparing the model slope, loading was applied using a plate that displaced vertically from the top of the slope at a constant rate of 1.0 mm/min to induce slope failure. The experimental results showed that the tilt angle increased as slope failure progressed, with the response of the angular velocity being particularly pronounced in the inclinometer located near the end of the shear band. The changes in angular velocities corresponded to the stages of slope failure described in previous studies. Furthermore, the angular velocity increased by a factor of about 10 as the slope transitioned from the elastic to the plastic region. Regarding the installation conditions of the inclinometers, shorter instrument lengths and shallower depths were more useful for detecting the location of the shear band and the onset of collapse.

**KEYWORDS:** Slope failure, inclinometers, angular velocity, monitoring.

## 1 INTRODUCTION

As the risk of landslides increases due to the increasing frequency of heavy rainfall in recent years, the development and introduction of advanced observation technologies are required to accurately assess slope conditions and ensure safety. Recently, a monitoring technique using surface inclinometers has been considered. This technique is expected to be a new slope monitoring technique that is highly compatible with DX, as it can observe slope dynamics by placing multiple points on the slope. The application of this technology to actual slopes and the accumulation of measurement data during slope failures have been steadily progressing, and observation systems have been proposed (Uchimura, 2015; Sheikh, 2021; Kawanami, 2024). Further accumulation of data and clarification of response characteristics are essential to improve the accuracy of slope monitoring technology using inclinometers and to promote its practical application. In this study, we conducted slope failure experiments on a model slope to clarify the response characteristics of surface inclinometers to the slope collapse process and investigated the influence of inclinometer installation conditions on their response.

## 2 OUTLINE OF MODEL EXPERIMENT

The experimental apparatus, as shown in Figure 1, consists of a soil container and a loading device. The steel container was 900 mm in length, 400 mm in height, and 200 mm in width. The sides of the container were made of acrylic, allowing for the observation of its contents. A loading jack located at the top of the container allows the loading plate to be displaced vertically at a constant rate. A model ground with a height of 200 mm and a slope of 25° was prepared in the container using the air-fall method. Dry Toyoura sand was used as the soil material, with a unit weight of 1.61 g/m<sup>3</sup>, corresponding to a relative density of 93%. The Toyoura sand has a particle density of 2.65 g/cm<sup>3</sup> and minimum and maximum dry densities of 1.36 g/cm<sup>3</sup> and 1.65 g/cm<sup>3</sup>, respectively. Five inclinometers, as shown in Figure 2(a), were installed perpendicular to the model slope. The inclinometers consisted of an accelerometer and a sleeve. The tilt angles of inclinometers were calculated using the formula in Figure 2(b). The inclinometers were installed at 50 mm

intervals, starting 100 mm from the top of the slope, as shown in Figure 3. The inclinometers are numbered No.1 to 5 in order from the top of the slope. The capacities of inclinometers No. 1 and 5 are 10 G, and No. 2, 3, and 4 are 1 G, respectively.

After the model ground was prepared, a loading plate with a length of 80 mm and a width of 200 mm was displaced vertically downward from the top of the slope at a relatively low rate of 1.0 mm/min to generate slip on the model slope. The vertical load was measured by a load cell installed on the loading plate. Loading and unloading were performed three times each before and after the vertical loads reached the maximum values. The cyclic loading was intended to confirm the difference in response of the inclinometers between the elastic and plastic regions of the model slope.

The experimental conditions are summarized in Table 1. To understand the influence of installation conditions on the response of the inclinometers, 6 cases were conducted, varying the instrument length  $L$  to 25 and 45 mm, and the depth from the slope surface  $D$  to 10, 20, and 30 mm.



Figure 1. Experimental apparatus.

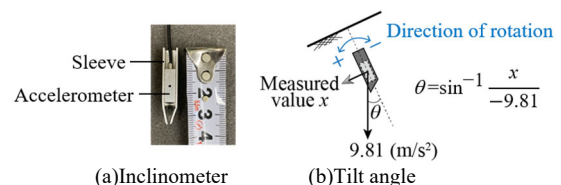


Figure 2. Inclinometer.

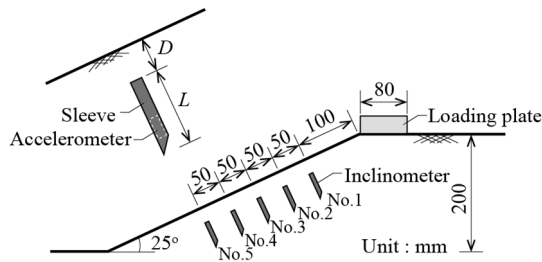


Figure 3. Installation conditions of inclinometers.

Table 1. Experimental conditions

Case	Length $L$ (mm)	Depth $D$ (mm)
L25D10		10
L25D20	25	20
L25D30		30
L45D10		10
L45D20	45	20
L45D30		30

### 3 RESPONSE OF INCLINOMETERS TO SLOPE FAILURE

The results for Cases L25D10 and L45D30 are discussed below to confirm the inclinometer response in the slope failure. Figures 4 and 5 illustrate the variation of loading stress, tilt angle, and angular velocity in each case. The loading stress was calculated as the vertical load divided by the area of the loading plate. The loading stress exhibited a typical behavior of the shear properties of dense soils, i.e., it gradually increased with the progression of loading, reached a peak, and then decreased to a constant value, except during cyclic loading. The peak value is referred to as the maximum loading stress, and the minimum value after the peak, excluding cyclic loading, is termed the minimum loading stress. The tilt angle during loading increased in a positive direction as loading progressed for all inclinometers. In other words, the inclinometers were tilted toward the toe of the slope. In Case L25D10, the tilt angles of inclinometers No. 1, 2, and 4 increase around the maximum loading stress, and particularly, the tilt angle of inclinometer No. 4 increases significantly. Uchimura et al. (2015) found that the tilt angles of inclinometers installed on the slope surface increase rapidly right before slope failure, based on the results from a rainfall experiment. If the time of maximum loading stress is regarded as the onset of slope failure, this experiment also captured the rapid increase in tilt angle at the beginning of failure. Figures 6 and 7 show the model slopes after the experiments in each case. The initial position of inclinometers and the position of the shear band are illustrated in the photographs. In both cases, inclinometer No. 4, which showed a significant increase in tilt angle, was located at the intersection with the shear band and near the point where the shear band terminated at the slope surface. The inclinometers rotate, therefore suggesting the presence of a shear zone, which indicates the shear band. The other inclinometers do not rotate, therefore indicating more dominant translation movement as the soil moves in rigid body motion. At this point, in Case L25D10, the reason why inclinometers No. 1 and 2 showed an increasing trend in tilt angle earlier than inclinometer No. 4 is likely due to the progression of failure. As mentioned above, inclinometer No. 4 was located at the end of the shear band. After the loading stress reached its maximum value, strain localization occurred. During this process, the change in tilt angle at inclinometers No. 1 and 2, which were not on the shear band, subsided. In contrast, the tilt angle at inclinometer No. 4, which is located at the end of the shear band, increased rapidly.

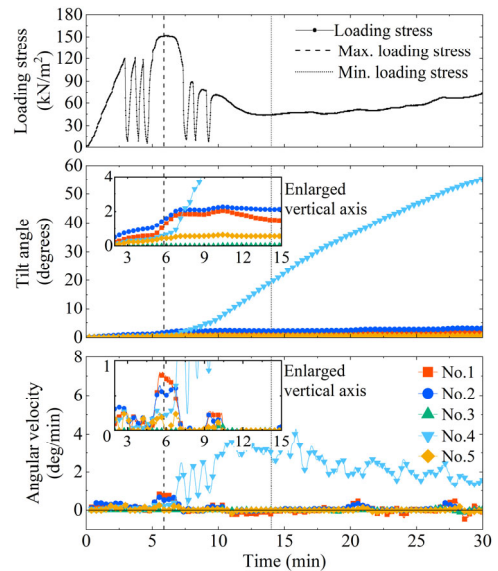


Figure 4. Variation of loading stress, tilt angle, and angular velocity. (Case L25D10)

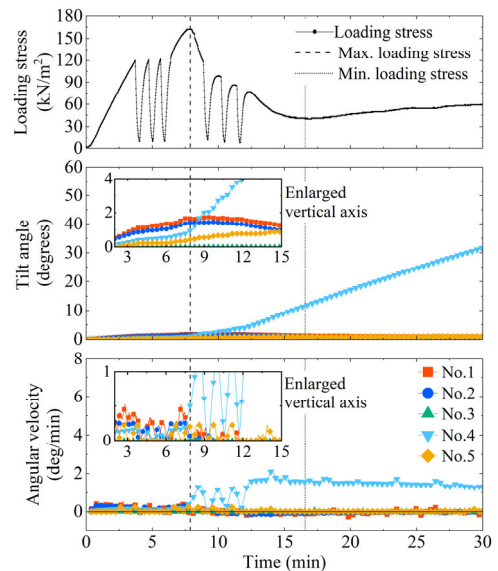


Figure 5. Variation of loading stress, tilt angle, and angular velocity. (Case L45D30)

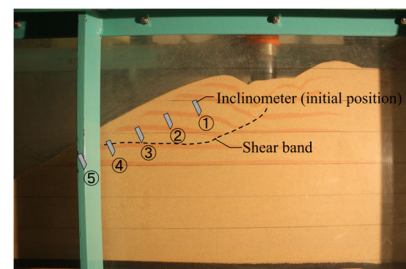


Figure 6. Model slope after the experiment. (Case L25D10)

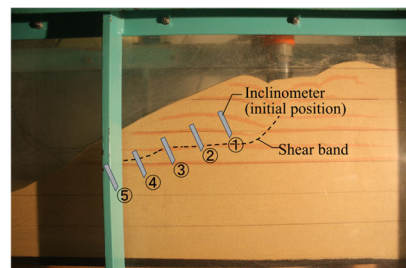


Figure 7. Model slope after the experiment. (Case L45D30)

Previous studies proposed slope hazard assessments based on the angular velocity measured by surface inclinometers (Uchimura, 2015; Sheikh, 2021). In this study, angular velocities were calculated from the tilt angle at each time and the angle 10 seconds before that time. As shown in Figures 4 and 5, the angular velocity at the initial stage of loading was about 0.2 deg/min. Within the cyclic loading process before reaching the maximum loading stress, the angular velocity decreases to 0 deg/min, but returns to approximately the original angular velocity during unloading and reloading, respectively. Around the time of the maximum loading stress, the angular velocities of inclinometers No. 1, 2, and 4 increased rapidly in Case L25D10, and especially inclinometer No. 4 reached 4.0 deg/min. In Case L45D30, the angular velocity of inclinometer No. 4 also increased near the time of the maximum loading stress, reaching approximately 2.0 deg/min. After the maximum loading stress is reached, the angular velocity of inclinometer No. 4 reaches an approximately steady-state condition. This is because the slope failure continued to progress after the maximum loading stress, even in the unloaded condition. These results indicate that the response of angular velocity changes significantly before and after the maximum loading stress.

Sheikh et al. (2021) proposed a classification system for slope movement based on the monitoring results of an unstable in-situ cut slope. When the angular velocity exceeds 0.004 deg/h, the “warning” level is alerted, indicating the slope has started to move. When the angular velocity exceeds 0.04 deg/h, the level indicates “evacuation”. Based on an analysis of embankment failure cases, Kawanami et al. (2024) proposed threshold values for angular velocity: when it exceeds 0.01 deg/h, slope failure may have already initiated and deformation is likely, which they define as the “field inspection level”; when it exceeds 0.05 deg/h, slope deformation is visibly apparent, corresponding to the “emergency response level.” The angular velocities obtained in this experiment were significantly higher than those reported in previous studies. This can be attributed to the constant loading rate of 1.0 mm/min, the use of dry sand, and the model-scale conditions of the experiment. However, the sharp increase in angular velocity, from 0.2 deg/min in the early stage of loading to over 2.0 deg/min after the maximum loading stress was exceeded, represents more than a tenfold change, which is a characteristic also reported in previous research.

Saito (1987) assumed that slope failure consists of three stages of failure: (i) the strain of soil increases, (ii) it grows at a constant rate, and (iii) it increases rapidly until failure occurs. Tamate et al. (2013) conducted a large-scale model experiment and observed three stages of failure based on the measured shear strain near the slope surface. The following sections discuss the correspondence between the tilt angle obtained in this study and the failure stage of the slope. Figure 8 shows the change in tilt angle and angular velocity for Cases L25D10 and L45D30. Only the results of inclinometer No. 4 are shown in Figure 8 for both cases. The horizontal axis indicates the time elapsed from the maximum loading stress in each case. The tilt angle increased slowly to about 1° from 0 minutes, the time of maximum loading stress, and then increased rapidly. This is considered to be a result of the elastic behavior of the ground before the maximum loading stress and the plastic behavior of the ground after the maximum loading stress. The angular velocity also increases significantly near the time of the maximum loading stress. If the angular velocity in the elastic region is denoted as  $\dot{\theta}_e$ , then the angular velocity  $\dot{\theta}_p$  observed in the plastic region showed a change approximately ten times greater than  $\dot{\theta}_e$ . The comparison between changes in angular velocity and the slope failure stages identified in previous

studies shows that the period from the start of loading until the angular velocity reaches a certain level corresponds to the first failure stage. The stage during which the angular velocity remains approximately constant, except during unloading, corresponds to the secondary failure stage. The phase where the angular velocity increases further corresponds to the third failure stage. These findings indicate that the slope angle reflects the elastic and plastic behavior of the ground, and that angular velocity exhibits distinctive patterns associated with each failure stage of the ground.

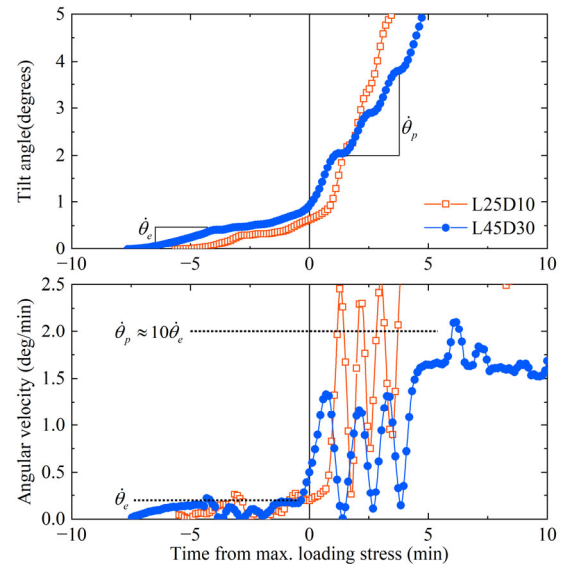


Figure 8. Tilt angle and angular velocity before and after maximum loading stress. (Inclinometer No. 4)

#### 4 EFFECT OF LENGTH AND DEPTH ON INCLINOMETER RESPONSE

The following is a comparison of results between cases to examine the effect of instrument length  $L$  and depth from the slope surface  $D$  on the inclinometer response. As mentioned above, inclinometer No. 4, both in Cases L25D10 and L45D30, showed significantly large angular velocities, and it was located across the shear band and close to the end of the shear band on the slope surface. Each of the other experimental cases also had inclinometers that exhibited particularly large angular velocities. Figure 9 shows the data of the inclinometers that exhibited the largest angular velocity in each case. In all cases, there was a sharp increase in angular velocity around the time of the maximum loading stress. Comparing the length of the inclinometer, the angular velocity after the maximum loading stress was greater for  $L=25$  mm than for  $L=45$  mm. This may be because the shorter length of the inclinometer can more easily follow the movement of the shear failure in the model ground. Only the angular velocity of Case L25D30 decreased to around 0 deg/min after the maximum loading stress. In this case, a shear band was observed to have developed just below the inclinometer, whose response is shown in Figure 9. The angular velocity decreased because the shear band formed below the inclinometer during the localization of strain due to slope failure progression.

One of the purposes of installing inclinometers is to detect signs of slope failure. Therefore, we examined how long before the onset of slope failure the increase in angular velocity, which is characteristic of slope failure, appears. Figures 10 and 11 show the angular velocities around the maximum loading stress for each experimental case. In all cases, the angular velocity increases slightly before the maximum loading stress. The value

at which the angular velocity begins to increase is set to 0.5 deg/min. The points indicated by the black arrows on the graph are considered to be the beginning of the angular velocity increase for each case. Figure 12 shows a summary of the time to reach 0.5 deg/min for each case. In the case of  $L=25$  mm, the shallower the insertion depth, the faster the increase in angular velocity begins. In the case of  $L=45$  mm, there was no clear relationship between insertion depths, with the fastest increase in velocity occurring at  $D=20$  mm. The mean time for the onset of angular velocity increase was -0.37 minutes for  $L=25$  mm and -0.16 minutes for  $L=45$  mm, indicating an earlier onset of angular velocity increase for  $L=25$  mm. The reason for this is thought to be that the shorter the instrument length, the more sensitive it is to the ground motion.

In conclusion, under the present experimental conditions, the shorter the instrument length  $L$  and the shallower the insertion depth  $D$ , the greater the angular velocity of the inclinometer and the earlier the rapid increase in angular velocity, a sign of slope failure, appears.

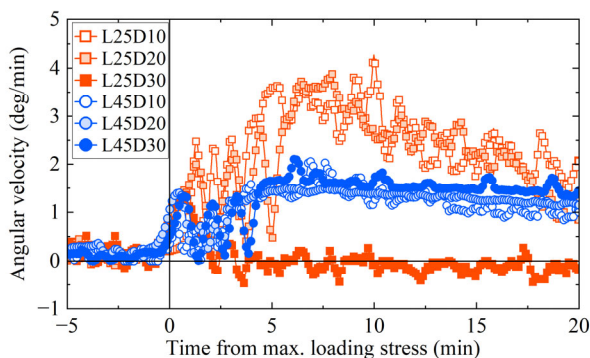


Figure 9. Comparison of the largest angular velocity responses.

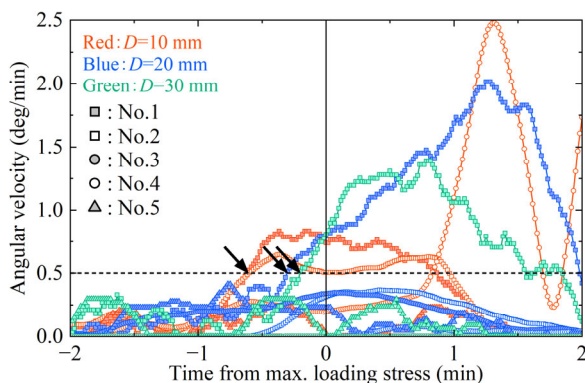


Figure 10. Angular velocity before and after maximum loading stress. ( $L=25$  mm)

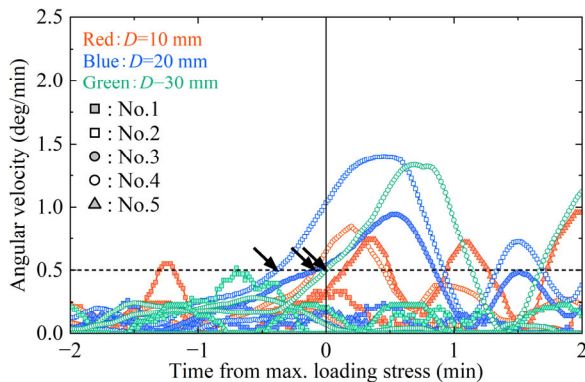


Figure 11. Angular velocity before and after maximum loading stress. ( $L=45$  mm)

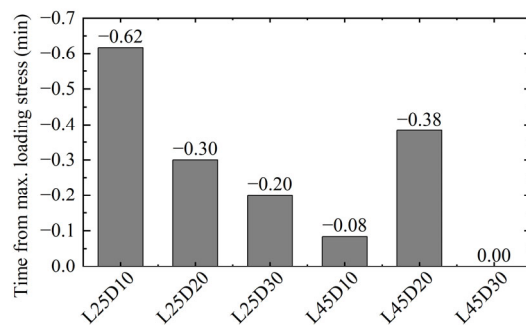


Figure 12. Time to reach 0.5 deg/min from maximum loading stress.

## 5 CONCLUSIONS

In this study, a model slope failure experiment was conducted to understand the response characteristics of surface inclinometers during a slope failure and to understand the effects of installation conditions on the response of inclinometers. The experimental results showed that the tilt angle and angular velocity increased with the progress of the slope failure, and the increase was especially significant for the inclinometer near the end of the shear band at the slope surface. The tilt angle showed a response that corresponded to the elastic and plastic behavior of the ground, and the angular velocity changed by a factor of about 10 as the slope transitioned from the elastic to the plastic region. Furthermore, under the conditions of this experiment, it was found that the shorter the instrument length and the shallower the insertion depth, the more useful it was for locating the end of the slip surface and for identifying signs of collapse.

This experiment was conducted using a model-scale slope made of dry sand. The experimental results cannot be directly applied to actual field conditions. However, the experiment allowed for a qualitative understanding of responses such as angular velocity in relation to slope failure. These findings will serve as fundamental data for establishing a method to evaluate slope stability using inclinometers in the future.

## 6 ACKNOWLEDGEMENTS

The authors would like to express their sincere gratitude to Mr. Kawanami and Mr. Hirai of West Nippon Expressway Engineering Chugoku Co., Ltd, and Mr. Miyazaki and Mr. Nemoto of OYO Corporation for providing valuable information on inclinometers and for their insightful comments on this research. We also thank Mr. Fukuda and Mr. Amano, former students at Yamaguchi University, for their contribution to conducting the experiments and analyzing the data.

## 7 REFERENCES

- Uchimura, T., Towhata, I., Wang, L., Nishie, S., Yamaguchi, H., Seko, I., and Qiao, J. 2015. Prediction and early warning of surface failure of slopes using tilt sensors, *Soils and Foundation* 55(5), 1086-1099.
- Sheikh M.R. et al. 2021. Rainfall-induced unstable slope monitoring and early warning through tilt sensors, *Soils and Foundation*, 61(4), 1033-1053.
- Kawanami, T. et al. 2024. Collapse behavior of affected embankments with surface inclinometer, and proposals of new observation system, *Ground engineering*, 42(1), 81-87.
- Saito, M. 1987. On application of creep curves to forecast the time of slope failure, *Landslides*, 24(1), 30-38.
- Tamate, S. et al. 2013. A large scale model test on detection of potential risk of slope failure by monitoring of shear strain in shallow section, *Journal of Japan Society of Civil Engineers, Ser. C (Geosphere Engineering)*, 69(3), 326-336.